

**MINT 709 – Capstone project**

**Spectrum Sensing with Improved Energy Detector  
under Uncertain Noise Variance**

**Prakash Jayachandran**

E-mail: [pjayacha@ualberta.ca](mailto:pjayacha@ualberta.ca)

**Submitted to:** Dr. Mike McGregor

Professor and Chair

Department of Computer Science

Supervisor

Vesh Raj Sharma Banjade

Department of Electrical & Computer Engineering

University of Alberta

February 17, 2014

## **Abstract**

Spectrum sensing (detection of spectrum holes) in cognitive radios (CRs) has been a promising technique to alleviate the problem of radio frequency (RF) spectrum scarcity. Among several available techniques to detect the availability of spectrum holes, the energy detector (ED) has been one of the most popular methods due to its ease of implementation and non-coherent nature. However, the energy detector is suitable only when the noise variance is known with absolute certainty, and its performance starts degrading with an increase in noise variance uncertainty. Motivated by this fact, we use an improved energy detector (IED), which is a more generalized version of the ED, to mitigate the problem of noise variance uncertainty by adaptively tuning one of its critical parameters of interest. Our results show that a significantly better performance than that of the ED can be obtained by using a single CR based on an IED. To further enhance the spectrum sensing performance, the scenario is extended to cooperative spectrum sensing where a number of CRs collaborate with each other to jointly identify any possible spectrum holes. The MAJORITY fusion rule is deployed at the fusion center (FC) to combine the independent decision from the CRs. Encouraging performance gains compared to those obtained by using the single CR based spectrum sensing are observed.

## Table Of Contents

<b>List of Figures</b> .....	<b>iii</b>
<b>List of Abbreviations</b> .....	<b>iv</b>
<b>List of Symbols</b> .....	<b>v</b>
<b>1. Introduction</b> .....	<b>1</b>
1.1 Motivation .....	1
1.2 Objectives.....	4
1.3 Problems.....	4
1.3.1 Performance of improved energy detector under noise variance uncertainty .....	4
1.3.2 Cooperative spectrum sensing with improved energy detector under noise variance uncertainty.....	5
<b>2. Literature review</b> .....	<b>6</b>
2.1 Radio frequency spectrum.....	6
2.1.1 RF Spectrum underutilization .....	6
2.1.2 Spectrum holes .....	7
2.2 Cognitive radio .....	7
2.3 Spectrum sensing.....	8
2.4 Energy detector .....	9
2.5 Hypothesis testing .....	10
2.5.1 Performance metrics .....	10
2.6 Improved energy detector.....	11
2.7 Fading channel models.....	12
2.7.1 Rayleigh fading .....	12
2.8 Cooperative diversity .....	12
2.9 Noise model.....	14
2.9.1 Gaussian noise.....	14
2.9.2 Additive white Gaussian noise.....	14
2.9.3 Noise Variance Uncertainty .....	15

<b>3.</b>	<b>Spectrum Sensing with Improved Energy Detector in Fading and Noise Variance Uncertainty .....</b>	<b>16</b>
3.1	System model.....	17
3.2	Simulation model.....	18
3.3	Description of simulation model.....	18
3.4	Numerical results and discussions .....	18
3.5	Conclusion .....	29
<b>4.</b>	<b>Conclusion and Future Work .....</b>	<b>30</b>
	<b>References.....</b>	<b>31</b>

## List of Figures

- Fig. 1. Increase in mobile data traffic forecast.
- Fig. 2. Spectrum utilization graph.
- Fig. 3. Spectrum holes.
- Fig. 4. Block diagram of an energy detector.
- Fig. 5. Block diagram of an improved energy detector.
- Fig. 6. Cooperative spectrum sensing in CR network.
- Fig. 7.  $P_e$  vs.  $p$  for different  $\rho$  with SNR =  $-10$ dB,  $\lambda = 6.9$  and  $N=10$ .
- Fig. 8.  $P_e$  vs.  $p$  for different  $\lambda$  with SNR=  $-10$ dB,  $N=10$  and  $\rho$  as  $0.9$ .
- Fig. 9.  $P_e$  vs.  $p$  for different  $N$  with  $\lambda =6.9$   $\rho = 0.2$  and SNR =  $-10$ dB.
- Fig. 10.  $P_d$  Vs. SNR for different  $\rho$  for  $p = 4$ ,  $\lambda = 6.9$  and  $N = 10$ .
- Fig. 11.  $P_e$  vs. SNR for different  $\rho$  for conventional energy detectors ( $p=2$ ),  $\lambda = 6.9$  and  $N = 10$ .
- Fig. 12.  $P_e$  vs.  $\lambda$  for different SNR with  $p = 4$ ,  $N$  of  $4$  and  $\rho$  of  $0.2$ .
- Fig. 13.  $Q_e$  vs.  $p$  for various  $K$ -values in cooperative spectrum sensing with  $\lambda = 6.9$ ,  $N$  of  $10$  and SNR =  $-10$ dB.
- Fig. 14.  $Q_e$  vs.  $p$  for different  $\rho$  in cooperative spectrum sensing with  $N$  of  $10$ , SNR =  $-10$ dB and  $\lambda = 6.9$ .
- Fig. 15.  $Q_d$  vs. SNR for different  $\rho$  in cooperative spectrum sensing with  $N$  of  $10$ ,  $\lambda = 6.9$  and  $p = 4$ .

## List of Acronyms

CR	Cognitive Radio
ED	Energy Detector
IED	Improved Energy Detector
SS	Spectrum Sensing
MFD	Matched Filter Detector
PU	Primary User
SNR	Signal to Noise Ratio
SU	Secondary User
CAGR	Computed annual growth rate
AWGN	Additive white Gaussian noise

## List of symbols

$K$	Number of cognitive radios
$P_e$	Probability of error
$Q_{md}$	Probability of misdetection in cooperative spectrum sensing
$Q_f$	Probability of false alarm in cooperative spectrum sensing
$P_d$	Probability of detection
$Q_e$	Probability of error in cooperative spectrum sensing
$Q_d$	Probability of detection in cooperative spectrum sensing
$p$	Positive arbitrary constant
$N$	Sampling size
$P_f$	Probability of false alarm

# Chapter 1

## Introduction

### 1.1 Motivation

An explosive growth in wireless services has occurred in the past few years. The resulting demand for an increased data rate has made the bandwidth even more precious and scarce than it was previously. The competitive trend among the service providers and the crowded nature of spectrum allocated to them illustrate this development. For example, Fig 1. shows the increase in mobile traffic in recent years.



Fig. 1. Increase in mobile data traffic forecast [12]

The Asia Pacific and North America regions will account for almost two-thirds of global mobile traffic by 2017, as shown in Fig. 2. The Middle East and Africa will experience the highest computed annual growth rate (CAGR) of 77 percent, an increase of 17.3-fold over the forecast period. The Asia Pacific region will have the second highest CAGR of 76 percent, an increase of 16.9-fold over the forecast period. The emerging market regions of Latin America and Central and Eastern Europe will have



CAGRs of 67 percent and 66 percent respectively, and combined with the Middle East and Africa will represent an increasing share of total mobile data traffic, up from 19 percent at the end of 2012 to 22 percent by 2017. Such enormous growth in the demand for wireless services will translate into a demand for an equivalent bandwidth requirement, which in turn depends upon the available radio frequency (RF) spectrum. However, the traditional spectrum allocation policy of several government agencies around the world allocates a specific portion of RF spectrum exclusively to a specific service. For example, all cellular phone networks worldwide use the portion of the spectrum designed as Ultra high frequency (UHF), i.e., from 300 MHz to 3 GHz and the same UHF is used for television, Wi-Fi and Bluetooth transmission. The users, who have an exclusive license to use a particular spectrum, are termed the primary users (PUs) of the spectrum.

However, studies have shown that the PUs are not always active and thus the allocated RF spectrum may be vastly underutilized across time and space. For example, a recent measurement conducted at the Berkeley wireless research center [1] is shown in Fig. 2., which shows the variation of the power spectral density across frequency. Clearly, the RF spectrum from 2 GHz to 6 GHz is hardly utilized. Also, a field spectrum measurement taken in New York City showed that the maximum total spectrum occupancy was only 13.1% from 30 MHz to 3 GHz [1].

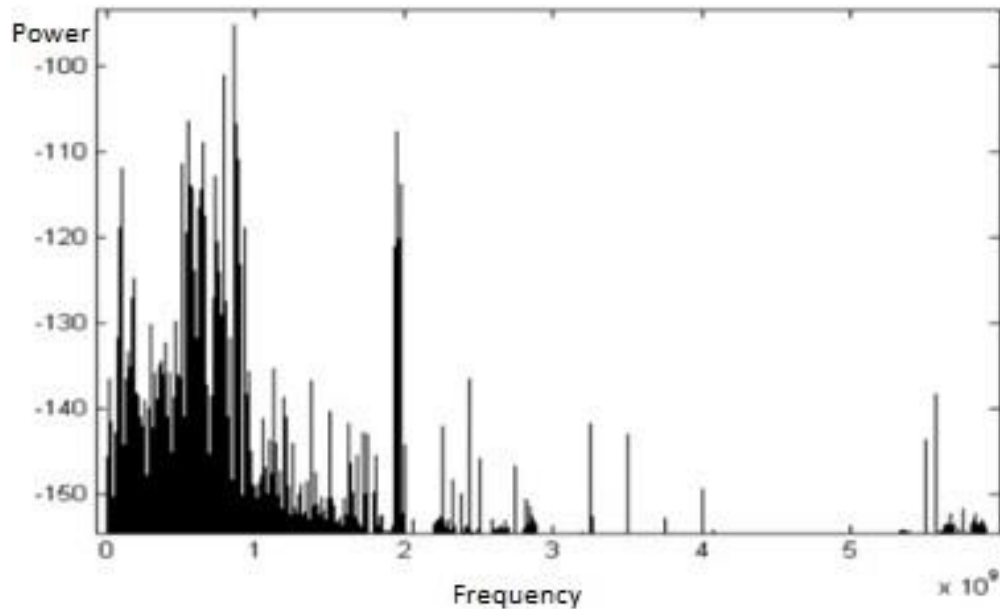


Fig. 2. Spectrum utilization graph [20]

Similar results were obtained in the most crowded areas of downtown Washington D.C., indicating less than 35% occupancy of the radio spectrum below 3 GHz [2].

Thus, a means to address the problem of this vast underutilization of the RF spectrum is needed. To increase spectrum utilization (spectral efficiency), a possible solution may be to identify the unused spectrum if it is successfully detected, it can be temporarily made available to some opportunistic users called the secondary users (SUs) of the spectrum. This allocation results in a demand for new technology to determine whether or not the spectrum is being used at any given time. In other words, it is necessary to “sense” the availability of communication opportunities, which are called as “spectrum holes” [5]. This process, popularly known as “spectrum sensing” in the literature, has led to the evolution of intelligent devices called cognitive radios (CRs) [1]. The foremost task of a CR is to continuously sense the spectrum to detect the reappearance of the PU in order to avoid harmfully interfering with the PU and, thus, to alleviate the problem of spectrum scarcity by promoting dynamic spectrum utilization.

Several spectrum-sensing techniques are popular in the literature, for example, the matched filter detector, cyclostationary-feature detector, wavelet-based detector, covariance-based detector and energy detector [4]. The energy detector (ED) is one of the most popularly used detection techniques due to its simplicity and non-coherent nature.

An ED computes the energy of a signal in the band of interest, compares this energy to a pre-determined threshold value, and decides whether the desired signal is present or not. The main advantage of an ED is that it does not require any knowledge of the signal such as the modulation format, symbol synchronization, design structure, decision-making and cost [3] and thus may be very suitable for blind spectrum sensing purposes. However, the nature of the channel between the PU and the sensor and, hence, the power of the received signal in relation to the noise level will impact the performance of an ED as it cannot detect the primary signal at a low signal-to-noise ratio (SNR) due to noise uncertainty. Although an ED performs well when the noise power is known with certainty, in reality, the noise power may vary with time, leading to noise variance uncertainty, so that the assumption of it being known or being estimated accurately is violated [13].

The ED performance is known to degrade under noise variance uncertainty [4]. Motivated by this fact, we consider a more generalized version of an ED in which the squaring operation on the received signal is replaced by an arbitrary power  $p > 0$  such that the ED is a special case  $p = 2$ . This detector is called the improved energy detector (IED) [4]. Numerical results show that the best power operation of the signal amplitude depends on the probability of false alarms, the probability of detection, the average signal-to-noise ratio (ASNR) or the sample size, but generally does not equal two as in the conventional energy detector [6]. Thus, it may be possible to compensate for the ED performance degradation due to noise variance uncertainty by considering an IED with adaptively tuned  $p$  value. Hence, we consider the IED in this study.

Next, the two main objectives of the project are briefly outlined in Section 1.2 and elaborated in Section 1.3.

## **1.2 Objectives**

1. Spectrum sensing with improved energy detector under uncertain noise variance and multipath fading environment.
2. Investigation of multiple antenna and cooperative spectrum sensing techniques to attain possible improvement in an ED under uncertain noise variance.

## **1.3 Problems**

The two objectives are now briefly elaborated as problems 1.3.1 and 1.3.2 respectively.

### **1.3.1 Performance of improved energy detector under noise variance uncertainty**

The spectrum sensing performance is adversely affected not only by noise variance uncertainty, but also by multipath fading, which is an inherent phenomenon in a wireless environment and occurs due to the nature of wireless signal propagation. Motivated by this fact, we need to effectively quantify the spectrum sensing performance of an IED in a joint scenario of multipath fading and noise variance uncertainty. Further, the possibility of obtaining performance gains compared to the performance of a traditional ED under these situations needs to be investigated.

### **1.3.2 Cooperative spectrum sensing with improved energy detector under noise variance uncertainty**

Another problem in spectrum sensing arises when a CR is shadowed from the PU due to the presence of large obstacles such as buildings or hills, such that the CR cannot effectively receive the PU transmit signal, thus giving rise to the hidden terminal problem [6]. In such a situation, the CR transmission will harmfully interfere with the PU transmission. Thus, cooperative spectrum sensing, in which a number of CRs collaborate with each other, is necessary in such a situation [14]. Moreover, the amount of performance gain that such a cooperative network of IED equipped CRs would yield relative to a single CR deploying the IED is an interesting topic for investigation.

## Chapter 2

# Literature Review

### 2.1 Radio Frequency Spectrum

The radio frequency (RF) spectrum is a range of frequencies from 3 kHz to 300 GHz used for wireless communications such as radio, television broadcasting, cell phones, satellite communications, wireless home networks, GPS and several other daily applications. However, all these applications cannot use the same range of frequencies as doing so results in interference. Hence, a different range of frequencies has to be allocated for different applications. For example, the frequency range from 54 to 806 MHz has been assigned for various television channels. (e.g. 54-72 MHz for television channel 2-69) [1] Within this frequency range, several service providers have to be allocated. These providers have to make sure that they do not violate federal regulations, which state that no service provider will access any licensed spectrum assigned for any other service provider, while also ensuring that all service providers meet the demands of wireless communication. These services providers have to make the best use of the allocated spectrum to provide services for customers, as neither the allocation nor the method of allocation will change. However, all these allocated spectrums are underutilized, and the service providers are left with no choice than to look for a new technology, that will provide the most effective use of the radio frequency spectrum.

#### 2.1.1 RF spectrum underutilization

A recent survey of spectrum utilization made by the Federal Communications Commission (FCC) has indicated that the actual licensed spectrum is largely underutilized in vast temporal and geographic dimensions [1]. Moreover, the spectrum usage varies significantly in various time, frequencies, and geographic locations [4]. As more users have switched from wired to wireless communication systems, an explosive growth in wireless communication is occurring. In order to meet this growth, the

underutilization has to be improved by utilizing the unused part (the spectrum holes) of the licensed band of the spectrum.

### 2.1.2 Spectrum holes

The CR enables dynamic utilization of a temporally unused spectrum, or the spectrum hole or white space [9]. A band of a spectrum can be considered unused if it can accommodate secondary transmissions without interfering with the primary user of the band. The region of the time-frequency-space in which a primary user allows a secondary user to utilize a channel is called a spectrum hole [5]. For example, in Fig. 3, a graph is plotted between the frequency and the time, with three frequency slots.

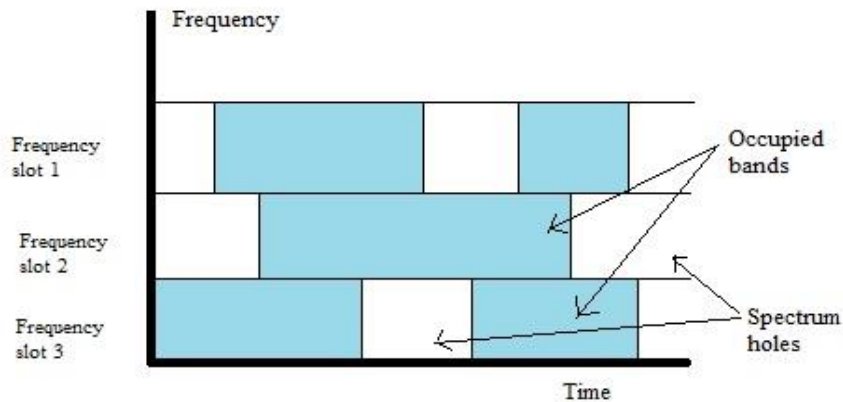


Fig. 3. Spectrum holes

Frequency slot 1 is completely vacant; in frequency slot 2, major portion of the spectrum is utilized, and the unused portion is the spectrum hole; and in frequency slot 3, the spectrum is not completely utilized, so between periods of use, it forms a spectrum hole. A secondary user can find an unused frequency band and utilize the band without interfering with the primary user. The spectrum sensing cognitive radio can sense these spectrum holes for better utilization of the radio frequency spectrum.

## 2.2 Cognitive Radio

Cognitive radio (CR) is the latest wireless communication technology that can monitor, sense and detect the conditions of its operating environment and dynamically reconfigure its characteristics to best match those conditions. The fundamental task of a

CR is spectrum sensing. However, the great improvement in the spectrum sensing CR, has helped it to sense the wireless channel and determine whether or not a PU is occupying the channel. When a PU does not occupy the channel, the SU can utilize the licensed spectrum until the reappearance of the PU. In order to detect the presence of the PU, the cognitive radio has to continuously sense the wireless channel to ensure the PU is being served without any interference from the secondary user. This process optimizes the use of the available RF. Apart from sensing the spectrum, CRs can also help in managing the spectrum and selecting the best available channel for the user. Spectrum sharing coordinates access to the channel along with other users [4].

### **2.3 Spectrum Sensing**

Spectrum sensing is the key factor in cognitive radio communication as this process senses spectrum holes to effectively use the radio spectrum. The main purpose of spectrum sensing is to detect the PU that is receiving data. The other purpose is to monitor the alternative empty spectrum in case the PU returns back to the spectrum being used by the SU. Once the primary user is detected, the switch to the secondary user from the channel becomes smooth. Several methods can be used to sense the spectrum, such as matched filter detection, cyclostationary detection, wavelet detection, covariance detection, and energy detector (ED). These methods are briefly explained below.

1) *Matched filter detection (MFD)*: is one of the common spectrum sensing techniques. In MFD, the SU needs to have a foregoing knowledge of the PU signal as it maximizes the SNR of the signal. The main disadvantage of MFD is that it requires the sensing receivers to be of different signal types [2]. Furthermore, its use is heavily dependent on the primary user signal, which is not available at CRs.

2) *Cyclostationary feature detection* is more resilient towards noise uncertainty, but requires previous knowledge of PU signal modulation format. An advantage of cyclostationary detection is the ability to operate at a very low SNR. The major disadvantages are some practical issues, such as the need for very long observation times, high computational complexity [4], and ultra-stable synchronization.

3) In *Wavelet-based detection*, an input signal is decomposed into different frequency components, and then each component is studied with resolutions matching its scale [4]. It can provide sharp changes and local features because of their basic functions that are irregularly shaped wavelets. However, its feasibility is limited by the need for high sampling rates, which are characterized by large bandwidths.

4) An *energy detector* (ED), also called a radiometer, provides a non-coherent method of detection. An ED computes the energy of a signal in a certain bandwidth [3] and compares this signal energy to a certain threshold value and decides whether the desired signal is present or not. The main advantage of an ED is that it does not require any knowledge of the signal such as the modulation format, symbol synchronization, design structure, decision-making and cost [3] and thus may be very suitable for blind spectrum sensing.

## 2.4 Energy Detector

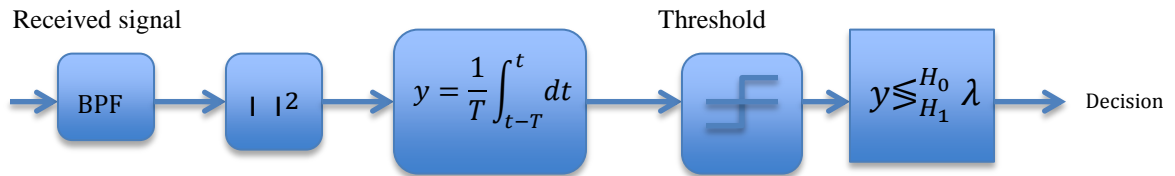


Fig. 4. Block diagram of an energy detector

An ED is also called a radiometer or a non-coherent detector. An ED simply computes the energy of a signal present in a certain bandwidth and compares it to a certain  $\lambda$  value to decide whether the desired signal is present or not. The resulting decision variable is then given by

$$T = \frac{1}{N} \sum_{i=1}^N |y_i|^2 \leq_{H_1}^{H_0} \lambda, \quad (2.1)$$

where  $\lambda$  is the detection threshold.



The main advantage of an ED is that it does not require any knowledge of the signal such as the modulation format or symbol synchronization. It has a simple design structure to perform real-time detection, and quick-sensing decision making and has a low cost [22]. As shown in Fig.4, an ED takes the input signal, passes it through a band-pass filter to select the bandwidth, and squares and integrates it over the observation period. The output is then compared with the predetermined  $\lambda$  to detect the presence of the PU.

## 2.5 Hypothesis Testing

The problem of PU signal detection can be modeled as a binary hypothesis-testing problem of the form [6]

$$X_i = W_i \quad : H_0 \quad (2.2)$$

$$X_i = S_i + W_i \quad : H_1, \quad (2.3)$$

Where,  $H_0$  (null) represents the hypothesis that the signal is absent;  $H_1$  (the alternate) represents the hypothesis that the signal is present;  $i = 1, 2, \dots, n$  signal samples;  $W_i$  is assumed to be white Gaussian noise with zero mean and variance,  $\sigma^2$ ; and  $S_i$  is the fading channel. The CR uses the following test statistic to make decisions about the presence or absence of the PU.

### 2.5.1 Performance metrics

The various performance metrics considered are the probability of detection ( $P_d$ ), probability of false alarm ( $P_f$ ), probability of error in decision making ( $P_e$ ), and the parameters of interest (SNR, sample size/time-bandwidth product,  $p$  – arbitrary positive constant, detection threshold ( $\lambda$ ), and number of CRs used in cooperative sensing). The probability of detection can be defined as the probability of detecting the PU in the channel and is given by

$$P_d = \Pr \{H_1 \text{ true} \mid H_0\} = \Pr \{T \geq \lambda \mid H_1\}. \quad (2.4)$$

The probability of a false alarm is given as the probability of detecting a user in the channel even though a user is not actually present:

$$P_f = \Pr \{H_1 \text{ true} \mid H_0\} = \Pr \{T \geq \lambda \mid H_0\}. \quad (2.5)$$

The probability of error ( $P_e$ ) is given as the chance of making a wrong decision by the receiver.

$$P_e = Pr\{H_0\} \cdot P_f + (1 - P_d)Pr\{H_1\}. \quad (2.6)$$

where,  $Pr\{H_0\}$  and  $Pr\{H_1\}$  are the probabilities of hypotheses  $H_0$  and  $H_1$  respectively.

## 2.6 Improved Energy Detector

An ED shows poor performance at severe noise variance uncertainty. Numerical results show that the best power operation of the signal amplitude depends on the probability of false alarm, the probability of detection, the average signal-to-noise ratio (ASNR) or the sample size, but generally does not equal to two as in the conventional energy detector [6]. Assigning a definite value for squaring the signal amplitude would hinder the correct process of detection.

$$T = \frac{1}{N} \sum_{i=1}^N |y_i|^p \quad (2.7)$$

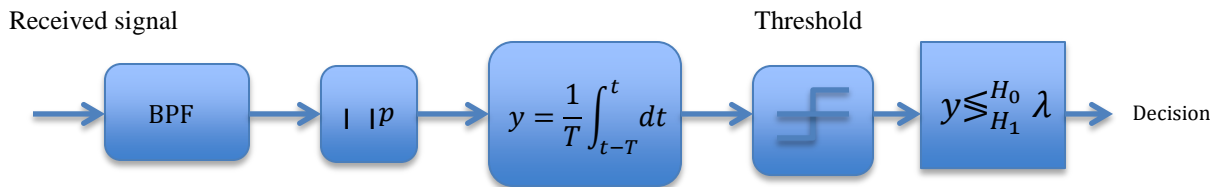


Fig. 5. Block diagram of an improved energy detector

An arbitrary value instead of a definite signal amplitude value improves an energy detector. An improved energy detector is proposed to detect the PUs under noise variance uncertainty. This is compatible with real world communications and would improve spectrum sensing performance, especially at low SNRs. Fig.5 is the block diagram of an improved energy detector [10].

## 2.7 Fading Channel Models

### 2.7.1 Rayleigh fading

The Rayleigh fading model is particularly useful in scenarios where the signal may be considered to be scattered between the transmitter and receiver. The Rayleigh fading model can be used to describe the form of fading that occurs when multipath propagation exists. In any terrestrial environment, a radio signal will travel via a number of different paths from the transmitter to the receiver. The most obvious path is the direct or line of sight path. When the signals reach the receiver, the overall signal is a combination of all the signals that have reached the receiver via the different available paths. These signals will all sum together, the phase of a signal being important. Depending upon how these signals sum together, the signal strength will vary [7]. Thus, the radio signal reaching the destination cannot be accurate. The Rayleigh fading channel probability density function is given as below:

$$f(x; \sigma) = \frac{x}{\sigma^2} e^{-\frac{x^2}{2\sigma^2}}, \quad x \geq 0, \quad (2.8)$$

### 2.8 Cooperative Diversity

The Cooperative spectrum sensing is considered in CR system to enhance the reliability of detecting the PU even under hidden terminal problem as tall building might shadow CRs. In this severe multipath-fading scenario, spectrum sensing is difficult. Due to these issues, CRs cannot detect the presence of the PU and this problem may result in interference [4]. In order to prevent these problems, multiple CRs are employed, and their decisions are sent to a fusion center where a final decision is made about the presence or absence of a primary user [23]. Fig. 6 demonstrates this process. The fusion center makes the final decision depending upon which fusion rule it uses.

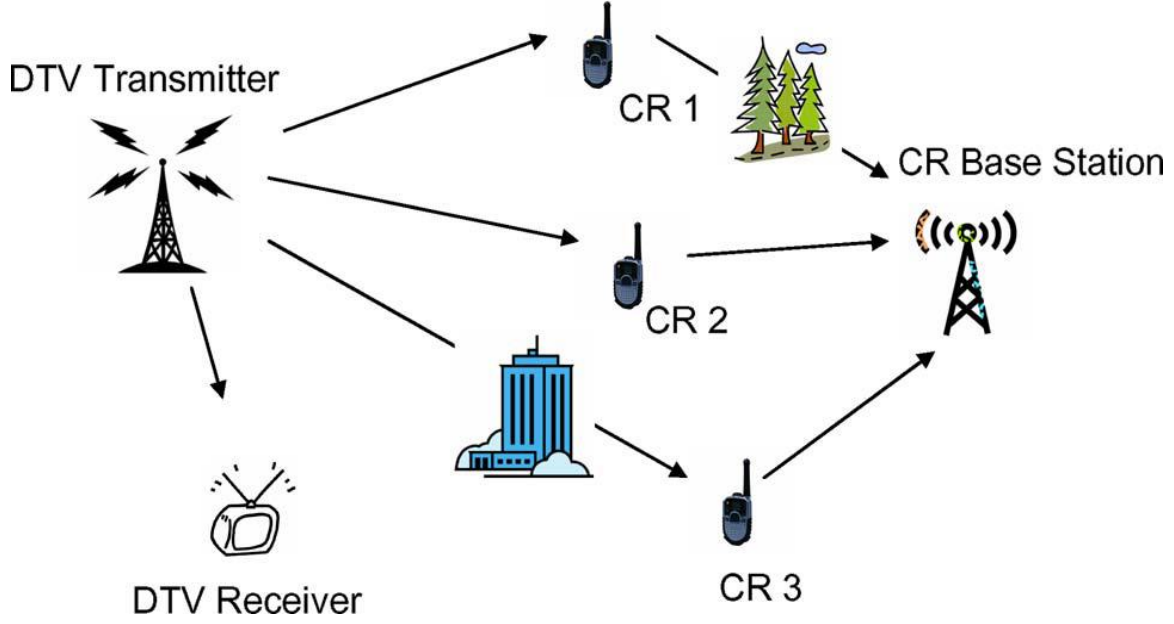


Fig. 6. Cooperative spectrum sensing in CR network [23]

The fusion rule has to be effective as it relies on several decisions made by an array of CRs. The two different types of fusion rules are the hard and the soft fusion rules. In case of soft fusion rule all the CRs forward the entire sensing result to the fusion center without performing any local decision. The decision is made between two hypotheses by taking linear combination of measurements of various CRs [25]. The second type of fusion rule is the hard fusion rule, when hard decisions are made, the AND, OR, MAJORITY, and  $N$ -out-of- $K$  methods can be used for combining the one-bit decision information regarding the existence of the PU from different cognitive radios [8]. In the AND-rule, all sensing results should be  $H_1$  for deciding  $H_1$ , where  $H_1$  is the alternate hypothesis, i.e. the hypothesis that a primary user is occupying the observed band. In the Or-rule, the fusion center decides  $H_1$  if any of the received decisions plus its own is  $H_1$ . In the Majority-rule, in order to decide  $H_1$  the majority of the nodes must have decision  $H_1$ . The  $N$ -out-of- $K$  rule (MAJORITY) outputs  $H_1$  when the number of  $H_1$  decisions is equal to or larger than  $N$  where there are a total of  $K$  cooperating nodes. The Majority rule is given by

$$Q_f = \sum_{l=n}^K \binom{K}{l} P_f^l (1 - P_f)^{K-l} \quad (2.9)$$

$$Q_m = 1 - \sum_{l=n}^K \binom{K}{l} P_d^l (1 - P_d)^{K-l}. \quad (2.10)$$

where  $P_d$  and  $P_f$  are probability of detection and probability of false alarm respectively.

Therefore, out of all the rules mentioned above, the majority rule is the most effective and reliable, as it considers the decisions of all the CRs in the system. In soft decision methods, the exact measurements are reported to the fusion center. which uses fixed weights for all the measurements reported to it. All received measurements are summed coherently and compared against one global threshold.

## 2.9 Noise Model

Noise is all around us in all sorts of forms like environmental/physical noise, semantic noise, external/internal noise and various other noises and can be the inherent fluctuations in some part of a system. Noise models are usually additive or multiplicative. Their type determines their classification into various forms. In this report, we are concerned mainly with the Gaussian model.

### 2.9.1 Gaussian noise

Gaussian noise usually does not depend on time and is always random, but its values at any pair of times are identically distributed and statistically independent and hence uncorrelated. Gaussian noise is a random noise and signals only the amplitude changes fluctuating randomly and its spectrum is totally different from that of Additive white Gaussian noise (AWGN). The probability density function ‘P’ of a Gaussian noise is given as below:

$$P_G(Z) = \frac{1}{\sigma\sqrt{2\pi}} e^{-\frac{(Z - \mu)^2}{2\sigma^2}}, \quad (2.11)$$

where  $\mu$  the mean value, and  $\sigma$  the standard deviation.

### 2.9.2 Additive white Gaussian noise

AWGN is a channel model in which the only impairment to communication is the linear addition of wideband or white noise with the constant spectral density (expressed

as watts per hertz of bandwidth) and a Gaussian distribution of amplitude. The model does not account for fading, frequency selectivity, interference, nonlinearity or dispersion. However, it produces simple and tractable mathematical models, which are useful for gaining insight into the underlying behavior of a system before these other phenomena are considered.

### **2.9.3 Noise variance uncertainty**

For many detection methods, the receiver noise power is assumed to be known. However, the noise power level may change over time due to environmental conditions. The two types of noise uncertainty are receiver device noise uncertainty and environment noise uncertainty. The receiver device noise uncertainty is due to the nonlinearity of receiver components and the time-varying thermal noise in them [17]. The environment noise uncertainty is caused by the transmissions of other users, either unintentionally or intentionally. Any detector suffers from device-level uncertainties due to the non-linearity of various components and non-uniform, time-varying thermal noise, etc. However, the dominant source of uncertainty for a cognitive radio network is the potential interference from the transmissions of other opportunistic devices communicating within the same band [17].

## Chapter 3

# Spectrum Sensing with Improved Energy Detector in Fading and Noise Variance Uncertainty

The performance of any wireless communications system is adversely affected by multipath fading. The ED is not an exception. A number of studies in the past have characterized the performance of ED in fading channel [19], [26], [27], [28]. All of these studies report degradation in performance of the ED-based CR in multipath propagation environments. However, these studies assume a perfectly known noise variance at the detector. In practical situations, the noise variance is not constant and may change with time [13], [29] and thus the assumption of it being known perfectly is violated. Although the ED performance under noise variance uncertainty is considered in [22], the analysis is limited to the assumption of a large number of samples at the CR. However, acquiring a large number of samples may violate the agile sensing requirement for a CR and thus the assumption of a large number of samples at the detector may not always hold. Furthermore, not much attention has been given in the literature for improving the performance of the ED under noise variance uncertainty that may be very important in designing practical detection systems for spectrum sensing in CR networks.

Motivated by the aforementioned problem, in this chapter, we consider the IED, which is known to yield remarkable performance gains, compared to the traditional ED [6], [24]. Again, these studies present their analysis assuming a perfect knowledge of the noise variance at the detector. However, the performance of an IED in multipath fading and under noise variance uncertainty has not been investigated and thus is the focus of this chapter. We consider the PU-CR channel to be Rayleigh faded and incorporate the uncertainty in noise variance into the received signal model at the CR. The sensing performance of the IED is studied and quantified under different operating conditions characterized by various parameters of interest such as the tuning parameter  $p$ , detection threshold, SNR and the noise variance uncertainty factor. In order to further enhance the performance of a single CR, a number of cooperating CRs is considered

next. We consider the deployment of MAJORITY based fusion of the independent CR decisions. The effect of the number of CRs on the detection performance metrics and the interplay of different parameters of interest are characterized in the numerical results.

The rest of the chapter is organized as follows. In Section 3.1, the system model is reviewed. The simulation model is presented in Section 3.2. Useful numerical results and the corresponding insights are demonstrated and discussed in Section 3.3. Finally, the chapter is concluded with Section 3.4.

### 3.1 System model

After the received signal at the CR is noise-limited and sampled at an appropriate rate, the  $i$ -th received signal sample under the two hypotheses can be expressed as

$$y_i = \begin{cases} \sqrt{\bar{\gamma}/\rho} h \cdot S_i + n_i & : H_1 \\ n_i & : H_0 \end{cases} \quad (3.1)$$

for all  $i = \{1, 2, \dots, N\}$ , where  $\bar{\gamma}$  is the average SNR,  $0 < \rho < 1$  is the noise variance uncertainty and  $h$  is the Rayleigh fading channel coefficient, whose PDF of the envelope  $\alpha = |h|$  is given by

$$p_\alpha(\alpha) = \frac{\alpha}{b_0} \exp\left\{-\frac{\alpha^2}{2b_0}\right\}, \quad \alpha \geq 0, \quad (3.2)$$

where  $2b_0$  is equivalent to the average envelope power. The received signal is then fed to the input of the IED, which, after processing, yields the decision statistic of the form

$$T = \frac{1}{N} \sum_{i=1}^N |y_i|^p \underset{H_1}{\overset{H_0}{\leq}} \lambda, \quad (3.3)$$

where  $\lambda$  is the detection threshold. These equations are used in our simulations and thus form the basis for computing the single CR-based detector performance metrics such as the probability of detection ( $P_d$ ), the probability of missed detection ( $P_m$ ), the probability of false alarm ( $P_f$ ), and the probability of error ( $P_e$ ).

For cooperative spectrum sensing, a total of  $K$  CRs are assumed to be independently detecting the PU signal activity. The final decision making process requires each CR to forward its individual decision to the FC which is in charge of combining the received decisions and yielding a final decision on the presence or absence of the PU. The FC is assumed to deploy MAJORITY fusion rule which is more general (and practical) than the traditional OR and AND fusion rules. To characterize the overall spectrum sensing performance of the CR network, the



desired performance are: cooperative detection probability( $Q_d$ ), cooperative probability of false alarm ( $Q_f$ ) and the cooperative probability of error( $Q_e$ ). For MAJORITY rule, these metrics are related to the metrics for a single CR as [4]

$$Q_d = 1 - (P_m)^k \quad (3.4)$$

$$Q_f = 1 - (1 - P_f)^k \quad (3.5)$$

Based on (3.4) and (3.5), the overall probability of error in decision making can be evaluated as

$$Q_e = (1 - Q_d + Q_f)/2 \quad (3.6)$$

assuming that the two hypotheses are equally-likely.

### 3.2 Simulation model

#### 3.3 Description of simulation model

The system model is implemented in MATLAB. Exhaustive Monte-Carlo simulations up to  $10^5$  iterations are carried for generating the numerical results.

#### Rayleigh fading channel generation

With the assumption of a large number of planes waves arriving at the receiver, the received complex envelope can be expressed as a complex Gaussian random process of the form [7]

$$h(t) = h_I(t) + jh_Q(t) \quad (3.7)$$

where  $h_I(t)$  and  $h_Q(t)$  are independent and identically distributed zero-mean Gaussian random variables with normalized noise variance 1 and  $j = \sqrt{-1}$  is the imaginary unit. Then, the amplitude of  $h(t)$ , denoted by  $\alpha(t) = |h(t)|$  will be Rayleigh distributed with the PDF given in

$$f(x; \sigma) = \frac{x}{\sigma^2} e^{\frac{-x^2}{2\sigma^2}}, \quad x \geq 0, \quad (3.8)$$

#### 3.4 Numerical results and discussions

In this section, several graphical results are presented to characterize the spectrum sensing performance of the IED under noise variance uncertainty. Inter-relationship between the critical parameters of interest are illustrated and the performance of single CR-based as well as

multiple CR-based spectrum sensing is characterized. Next, we briefly describe the graphical plots presented in this section.

In  $P_e$  vs.  $p$ , where the  $P_e$  takes the Y-axis and  $p$ -values takes the X-axis, a graph is obtained for the different values of the noise uncertainty, and for the constant values for  $\lambda$  and  $N$ . The rest of the graphs have the same axis properties, but are plotted for different varying values like  $\lambda$  and  $N$ . In Figures 9 and 10, in order to obtain the optimal value of threshold, the  $P_f$  has to be 0.1, for constant values for  $N$ ,  $p$  and noise uncertainty. The final graph in this chapter is plotted for the  $P_e$  and  $\lambda$  for differing SNRs. In this section, we have generated various graphs such as graphs for  $P_e$  vs.  $\lambda$ ,  $P_e$  vs.  $p$ ,  $P_e$  vs. SNR with various factors constant. In all the graphs generated some parameters are kept constant, and a few other parameters are assigned as variables in order to study the performance under various conditions to obtain the optimal  $p$  value and how they perform under very low SNRs and to compare the performance of conventional and improved energy detectors.

### ***Effect of $\rho$ on optimal $p$***

The effect of various levels of noise variance uncertainty on the optimal choice of the IED parameter  $p$  is illustrated in Fig. 7 with the help of a set of  $P_e$  vs.  $p$  graphs plotted for various  $\rho$  values. Several interesting observation can be made. First, it can be seen that the minimum  $P_e$  is obtained only at a particular value of  $p$  which is the optimal one since it maximizes the detection performance (lowest probability of error). Also, it is clear that the increase in noise variance uncertainty degrades the detection performance. Further, the optimal  $p$  changes with the change in  $\rho$ . In other words, to compensate for the degradation in detection performance due to increase in  $\rho$ , the parameter  $p$  needs to be changed adaptively to yield a minimum  $P_e$ . Another interesting observation is that beyond a specific  $p$  ( $p > 5.5$  in this case), the IED becomes independent of the noise variance uncertainty, i.e. the sensing performance remains the same. The last important observation is that as compared to the traditional ED, the  $P_e$  reduces significantly for the IED. For example, a reduction in  $P_e$  occurs by as much as 49 % when  $p$  is changed from 2 to the optimal value of 3.9 observed at  $\rho = 0.2$ . Hence, the IED is remarkably effective in mitigating the impact of noise variance uncertainty on the spectrum sensing performance of the traditional ED.

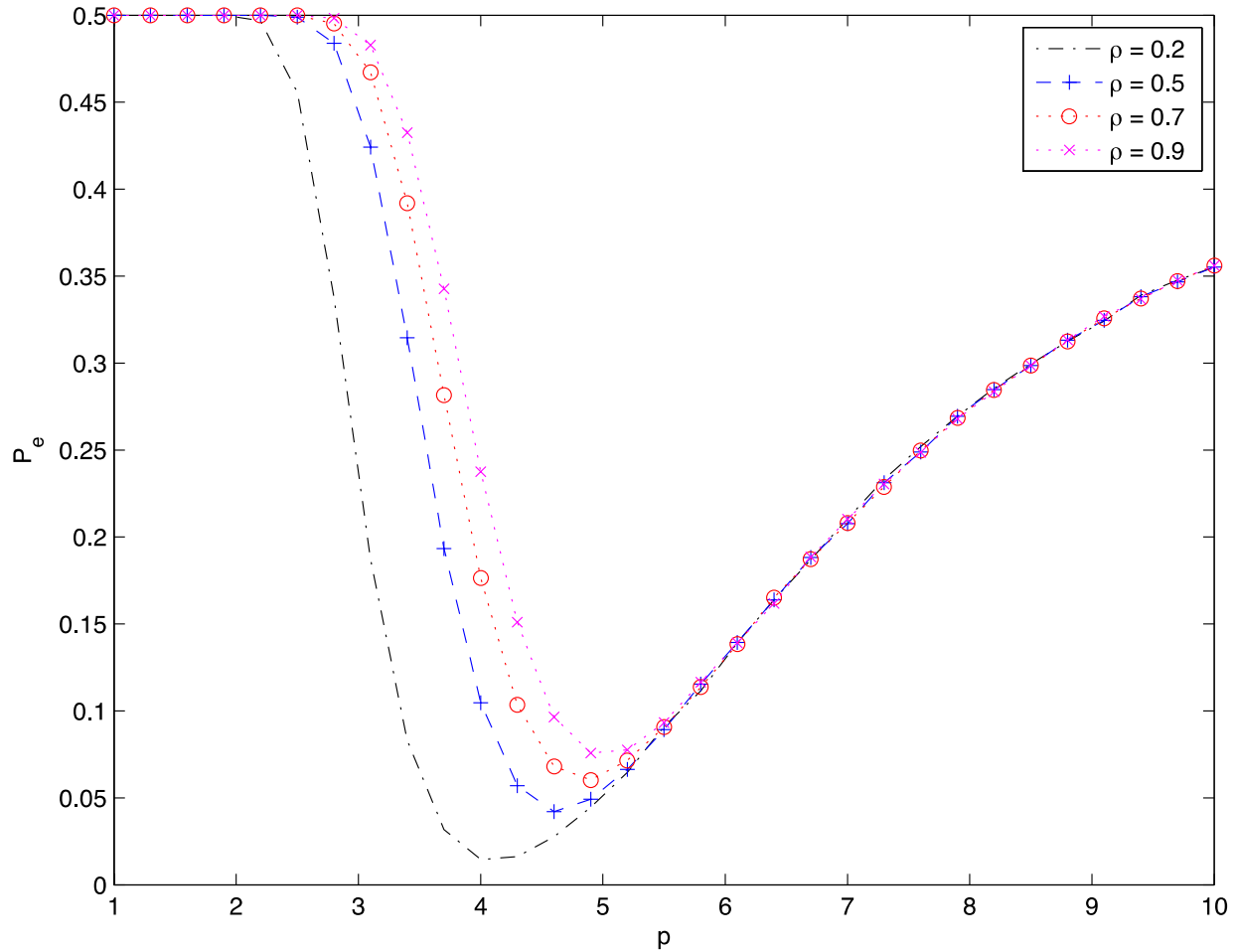


Fig. 7.  $P_e$  vs.  $p$  for different  $\rho$  with SNR = -10 dB,  $\lambda = 6.9$  and  $N = 10$ .

### ***Effect of $\lambda$ on optimal $p$***

Fig. 8 is a set of  $P_e$  vs.  $p$  graphs plotted for various values of  $\lambda$  values. It shows that, the minimum  $P_e$  is obtained only at a particular value of  $p$  that is the optimal one since it maximizes the detection performance. It is also noticed that higher values of  $\lambda$  increases the detection probability. Thus the optimal value of  $p$  changes with change in  $\lambda$ . But the optimal value with very low  $P_e$  could be attained for high values of  $\lambda$ . For example, the  $P_e$  is high for the conventional energy detector and decreases immediately by 25% for  $\lambda = 1.5$

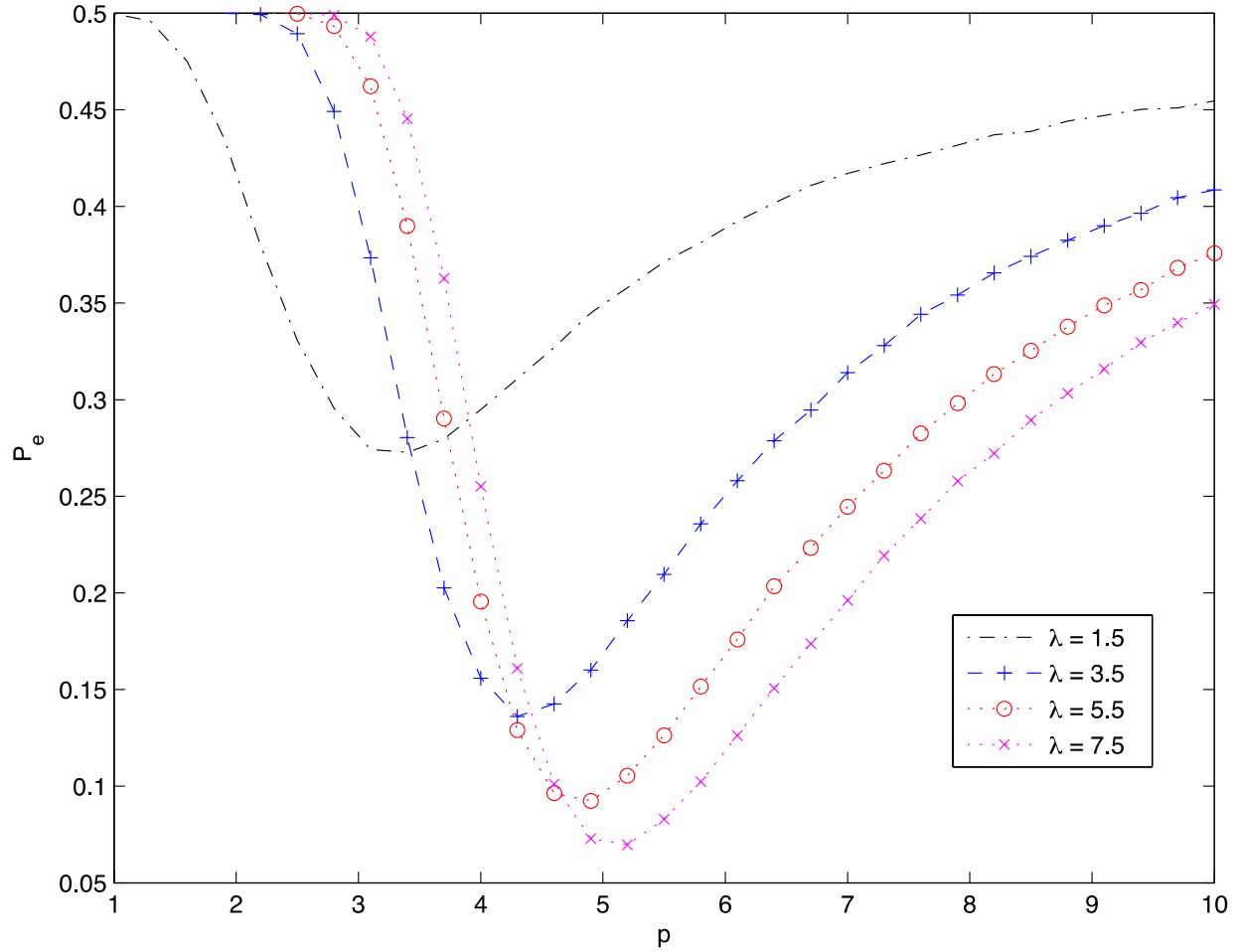


Fig. 8.  $P_e$  vs.  $p$  for different  $\lambda$  with SNR = -10dB,  $N$  10 and  $\rho = 0.9$ .

However, when the threshold value is increased by value of 2, the  $P_e$  is decreased to a minimum value for an optimal value of  $p = 5.2$  for a  $\lambda$  of 7.5. For the  $\lambda$  of 7.5, the  $P_e$  remains maximum until  $p = 3$  and falls suddenly to the minimum value. Thus, the optimal  $p$  value can be obtained from the range 3 to 5.2. The behaviour of the improved energy detector from the  $\lambda$  of 1.5 to 3.5 is notably different, after which this difference is negligible.

### ***Effect of $N$ on optimal $p$***

The influence of different values of sampling size on  $p$  is illustrated in Fig. 9 with the help of sets of  $P_e$  vs.  $p$  for different  $N$  values. Several observations are made in this graph. First, the minimum  $P_e$  is obtained only for a particular value of  $p$ , which is the optimal value too. It is also seen that increase in  $N$  value increases the detection probability. i.e., spectrum sensing

increases with an increase in  $N$  values. For lower values of  $N$ ,  $P_e$  decreases only until a certain point and remains with less difference for greater values of  $p$ , whereas when  $N$  increases, the  $P_e$  decreases to its minimum value and increases drastically beyond a certain point of  $p$ .

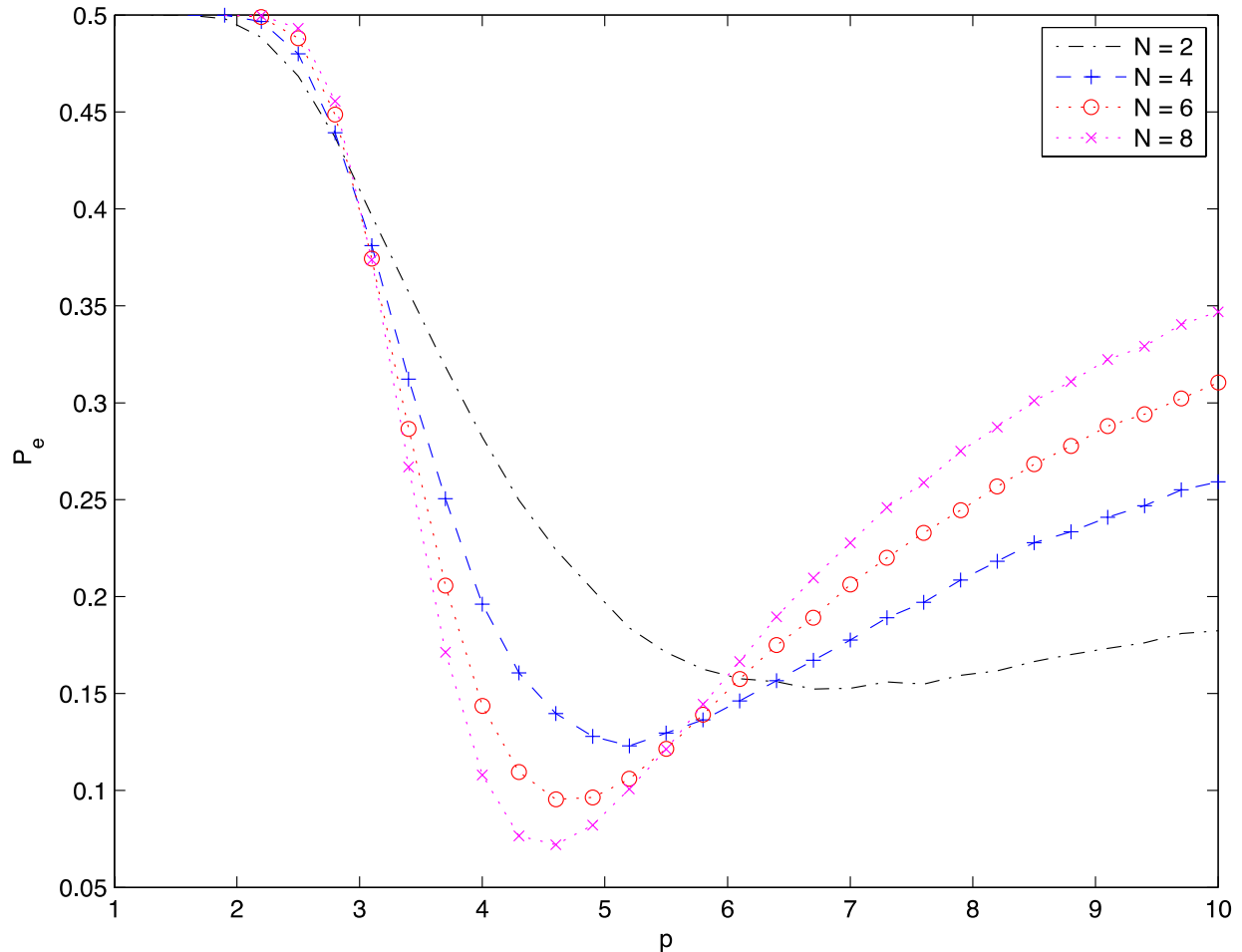


Fig. 9.  $P_e$  vs.  $p$  for different  $N$  with  $\lambda = 6.9$   $\rho = 0.2$  and  $\text{SNR} = -10\text{dB}$ .

The optimal value of  $p$  can be attained with higher values of  $N$ . For example, consider the graph, for the conventional energy detector ( $p = 2$ ), the  $P_e$  is independent of  $N$  values from 2 to 8, but when  $p$  increases slightly, there is a drastic change in  $P_e$ , and it is also noted that for greater values of  $N$ ,  $P_e$  reaches the minimum value of 7.2% for a  $p$  of 4.6. i.e.,  $N$  increases the probability of detection. For the lower sampling size values,  $N = 2$ , the minimum  $P_e$  that can attain is 17% at  $p = 6.7$ . However, in this case, the  $P_e$  does not decrease drastically unlike for high values of  $N$ . Thus, the  $P_e$  is minimum for the  $p$  values ranging from 4 to 5, and the optimal value of  $p$  can be obtained from the range of 4 to 5.

### Effect of $\rho$ on $P_d$ vs. SNR

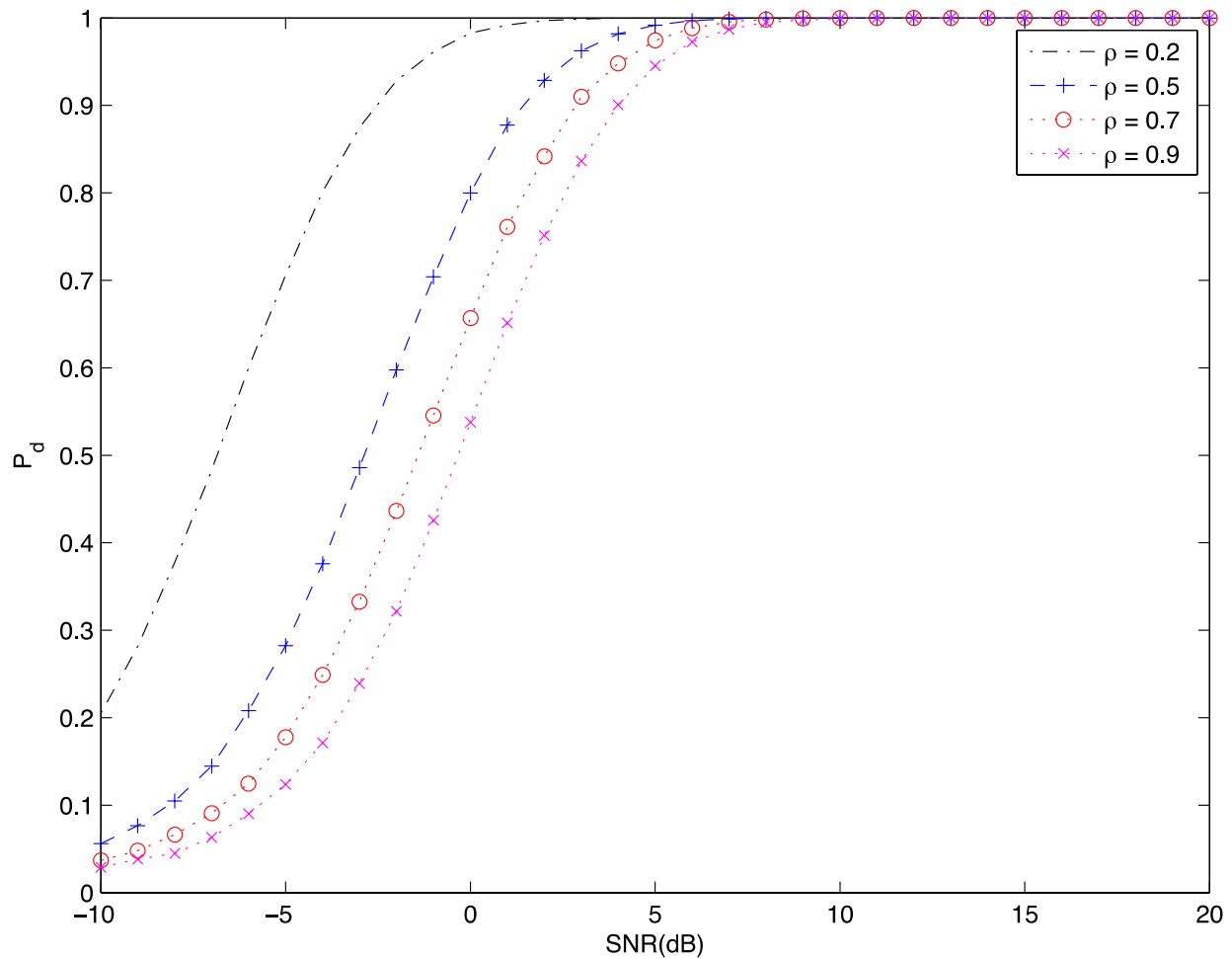


Fig. 10.  $P_d$  vs. SNR for different  $\rho$  for  $p = 4$ ,  $\lambda = 6.9$  and  $N = 10$

In general, in order to detect the PUs without any interference in the system, the system should be able to perform well even at the higher  $\rho$  values. In order to study the same, Fig.10 and Fig.11 are compared together and studied. Fig.10 is the  $P_d$  vs. SNR graph, in which the  $\rho$  varies for a conventional energy detector and Fig. 11 is the graph for  $P_d$  vs. SNR for different  $\rho$  in improved energy detector. In both these graph  $N$  and  $\lambda$  are considered constant. Fig.10 clearly reveals that the  $P_d$  is higher for a lower value of  $\rho$  and the  $P_d$  decreases as  $\rho$  increases at lower SNR values.

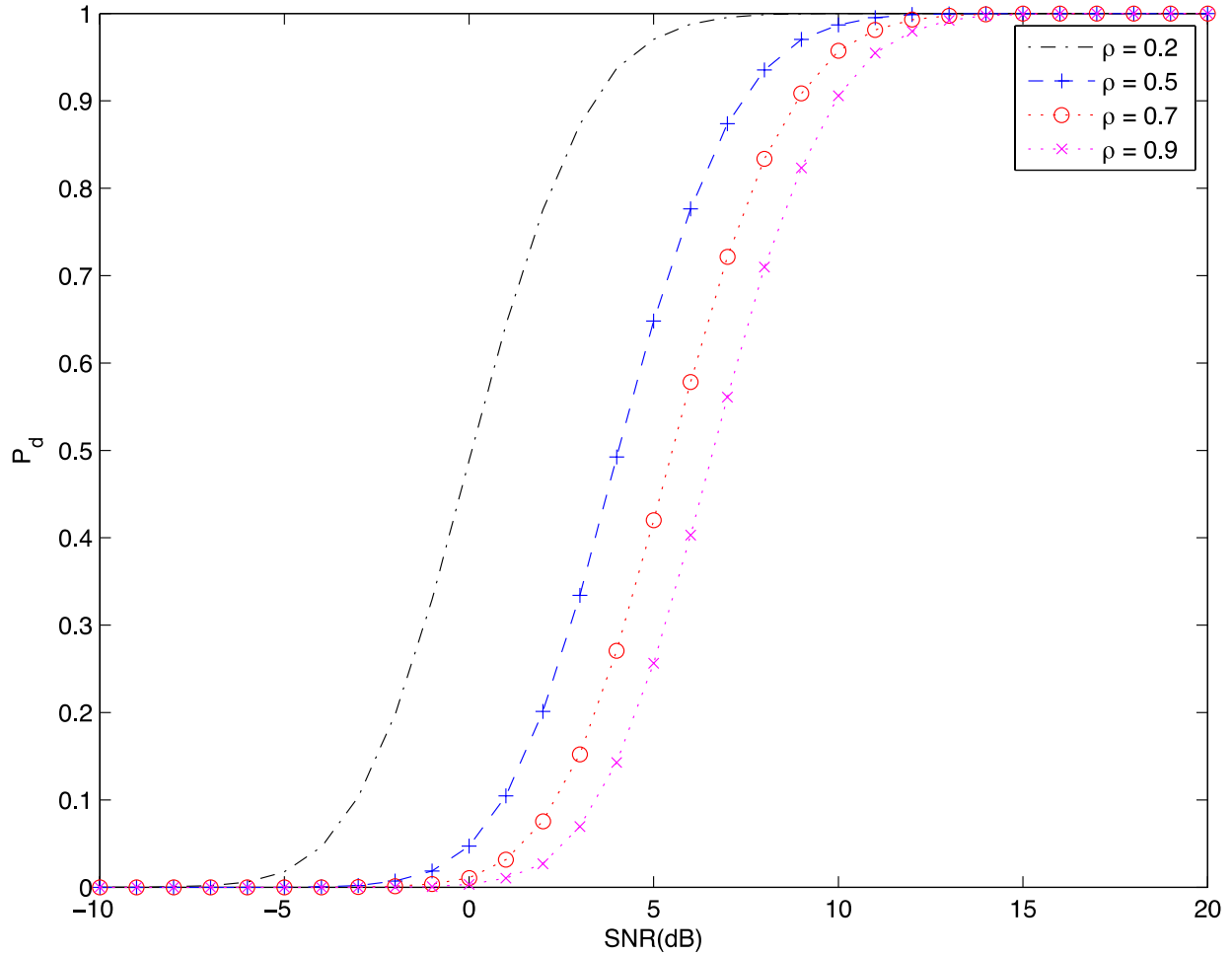


Fig. 11.  $P_e$  vs. SNR for different  $\rho$  for conventional energy detectors ( $p = 2$ ),  $\lambda = 6.9$  and  $N = 10$

For any of the  $\rho$ , the  $P_d$  is zero at the SNR level 0 dB in Fig. 10, whereas in Fig. 11, the  $P_d$  is 17% for the same value of the noise and the SNR. Both these graphs show that, for an increasing noise uncertainty level, the  $P_d$  is the same with increase in SNR value. The  $P_d$  attains 100% for the SNR value 6 dB, whereas in the conventional energy detector, a 6 dB gain interval of the SNR occurs with the improved energy detector compared to the performance of the conventional energy detector. Thus, in the improved energy detector, the  $P_d$  is possible even at low SNR values and with high noise uncertainty, with an increased efficiency of 50% more than that of the conventional energy detector.

### Effect of SNR on $\lambda$

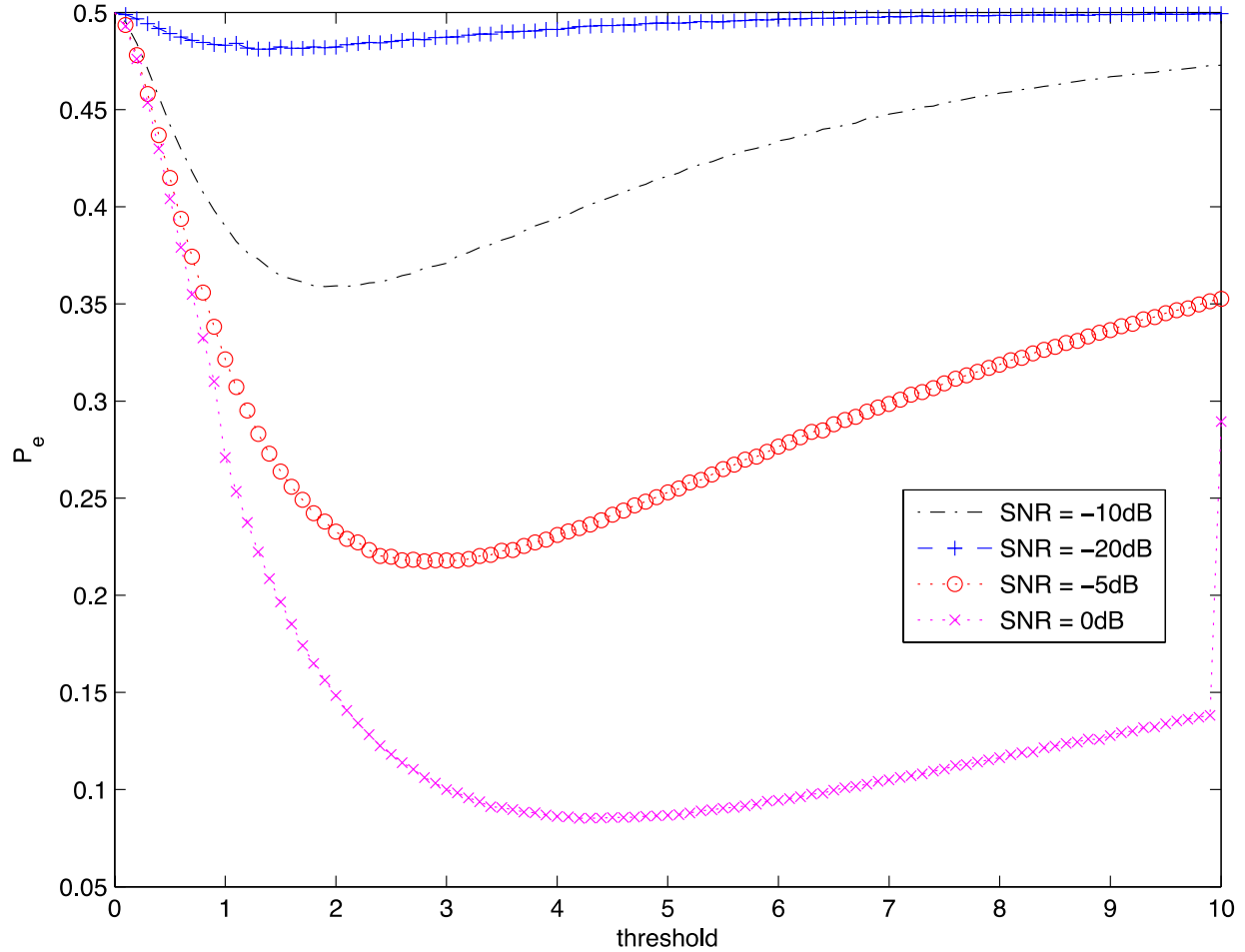


Fig. 12.  $P_e$  vs.  $\lambda$  for different SNR with  $p = 4$ ,  $N = 4$  and  $\rho = 0.2$ .

The effect of various SNR values on optimal  $\lambda$  is illustrated in Fig. 12. This figure clearly shows that, minimum value of  $P_e$  is obtained for a particular value of  $\lambda$  that is optimal one as it maximizes the detection probability. It is also clear from the graph that a very low value of SNR degrades the detection performance i.e., at very low values of the SNR, the  $P_e$  remains maximum and decreases when reach closer to 0db. The  $P_d$  is high for SNR values very close to 0db, and the optimal value of  $\lambda$  can be attained from the range -5 to 0. Fig.12 reveals that the  $P_e$  is 50%, or the maximum, for almost all the values of  $\lambda$  at -20dB, except in the range of 1 to 4. However, the  $P_e$  decreases drastically within a  $\lambda$  value of 0 to 2 and reaches the minimum value of 8.5% for a  $\lambda$  value of 4.2. Thus, the  $P_e$  decreases with an increase in the SNR, and the optimal  $\lambda$  value according to the graph is 4.2.



### Effect of $K$ on optimal $p$

The basic idea of Fig.13 is to study the number of CRs ( $K$ ) that should be used in the system to enhance the detection of PUs reliably. Fig. 13 is a set of  $Q_e$  vs.  $p$  for different numbers of CRs. Several interesting observations are made. First, there is a slight difference in optimal  $p$  value for different values of  $K$ , i.e., a slight difference occurs in the  $Q_e$  when  $K$  increases.

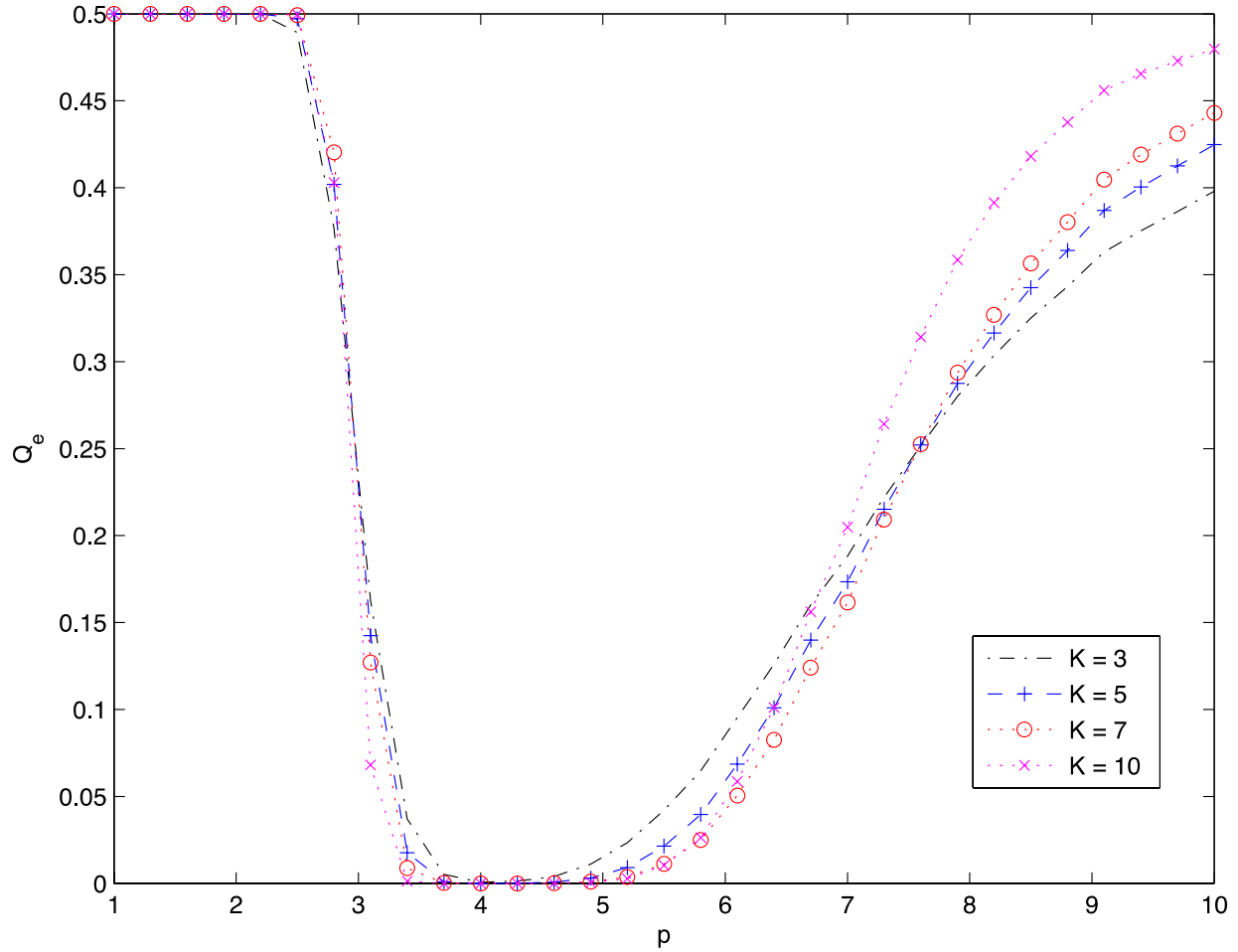


**Fig. 13**  $Q_e$  Vs.  $p$  for various  $K$  in cooperative spectrum sensing with  $\lambda = 6.9$ ,  $N$  of 10 and SNR = -10 dB.

The optimal value of  $p$  is clearly obtained in the range where the  $Q_e$  is minimum. This graph reveals that the  $P_e$  remains at a constant value of 50% for the conventional energy detector at a  $p$  of 2 and remains the same until  $p$  reaches 2.6. Beyond this  $p$  value, the  $Q_e$  plummets to 0.1% for a  $p$  of 3.4 and even reaches zero for a  $p$  of 4. This result implies that the cooperative spectrum sensing has a better performance. However, to figure out the number of CRs that need to be

involved in the system, the  $Q_e$  is considered for different  $K$ s at a fixed  $p$  of 3.7. For the improved energy detector with a  $p$  of 3.7, the  $P_e$  is 0.5% for  $K = 3$ . However, when the  $K$ -values are increased to 7 and 10, the  $Q_e$  becomes 0.02 and zero respectively. Thus, it can be concluded that performance of the system increases with an increase in number of CRs. However, the system performance degrades for a  $p$  above 6 for high  $K$  values. For these systems, the optimal  $p$  value should be considered in a range from 3.7 to 5.5.

### ***Effect of $\rho$ on optimal $p$***

Fig.14 is a set of  $Q_e$  vs.  $p$  graph plotted for various  $\rho$  values. One of the observations is that, for lower  $\rho$  the  $Q_e$  decreases drastically for a lower value of  $p$  and remains at its minimum until the point where there is no effect on the  $\rho$  values. When  $\rho$  increases, the  $Q_e$  decreases for slightly higher values of  $p$  and remains at its minimum until it has no effect on  $\rho$ . For example, the  $Q_e$  is maximum for conventional energy detectors and starts to descend quickly after a  $p$  of 2.5. The  $P_e$  is almost zero for a  $p$  of 3.7 at a noise uncertainty value of 0.2, while when  $\rho$  is 0.5, the  $Q_e$  decreases to zero only for a  $p$  of 4.3. From this comparison, it can be concluded that the system performance increases with a decrease in noise uncertainty. Another observation from this plot is that for any value of noise uncertainty, the  $Q_e$  is the same after a  $p$  of 4.6.

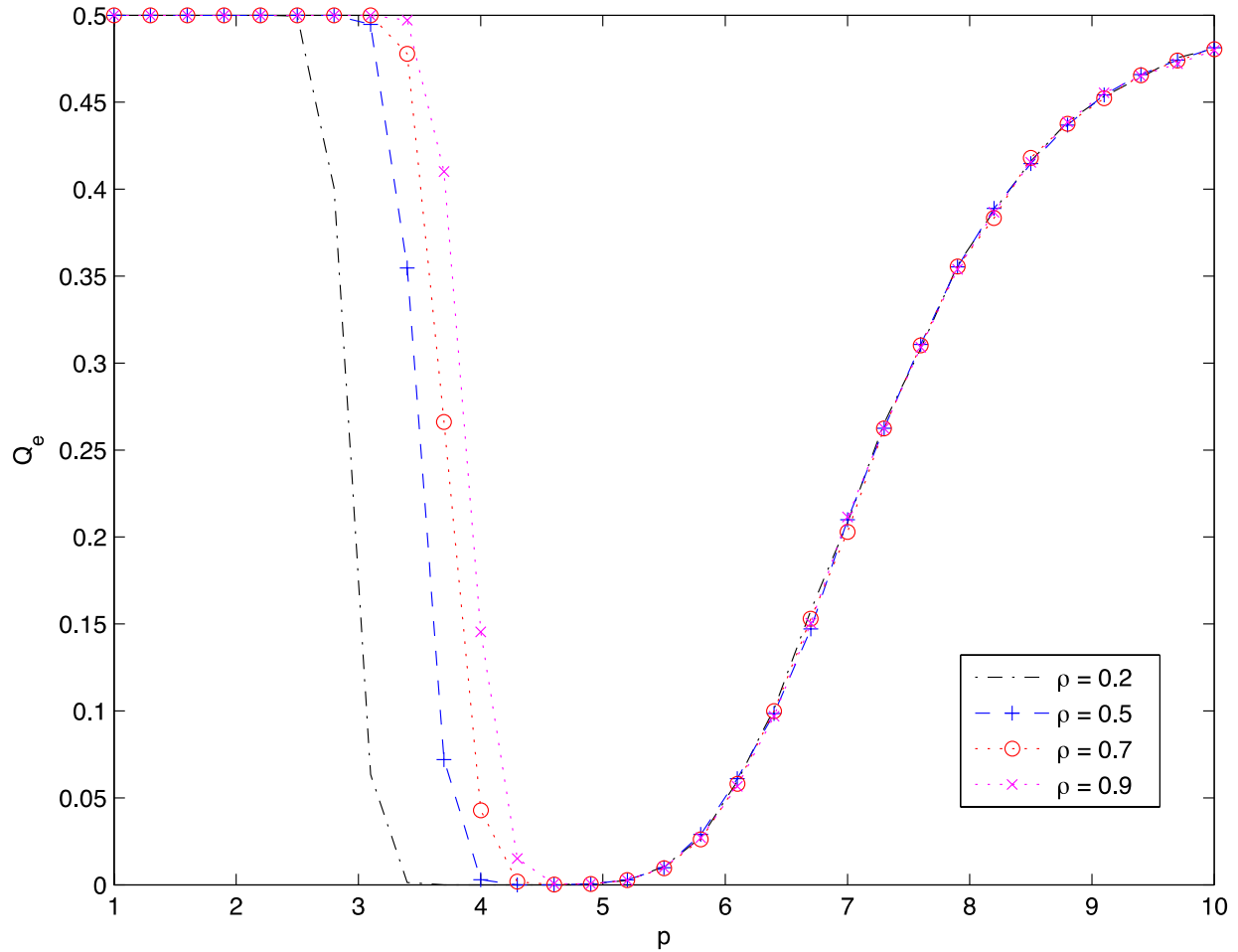


Fig. 14.  $Q_e$  Vs.  $\rho$  for different  $\rho$  in cooperative spectrum sensing with  $K = 10$ , SNR = -10 dB and  $\lambda = 6.9$ .

### Effect of $\rho$ on SNR

Fig. 15 is a graph to study the impact of different values of  $\rho$  on SNR. This could be studied with the help of a set of  $Q_d$  vs. SNRs for varying  $\rho$ . The graph shows that  $Q_d$  attains its maximum value for a low value of  $\rho$  at a lower SNR and when  $\rho$  increases,  $Q_d$  attains its maximum value only at higher values of SNR. We can also say that, the  $Q_d$  is high for low values of noise uncertainty. For example, the  $Q_d$  is 100% for a SNR of -4 dB and 100% at a SNR of 1 dB for  $\rho$  of 0.5. Secondly, when Figures 9 and 14 are compared, the  $Q_d$  is found to be 100% for SNR values of -4 dB and 0 dB with a  $\rho$  of 0.2. This result indicates that the performance of the improved energy detector is much better than that of the traditional energy detector in cooperative spectrum sensing, as the former can detect the PUs at much lower SNRs.

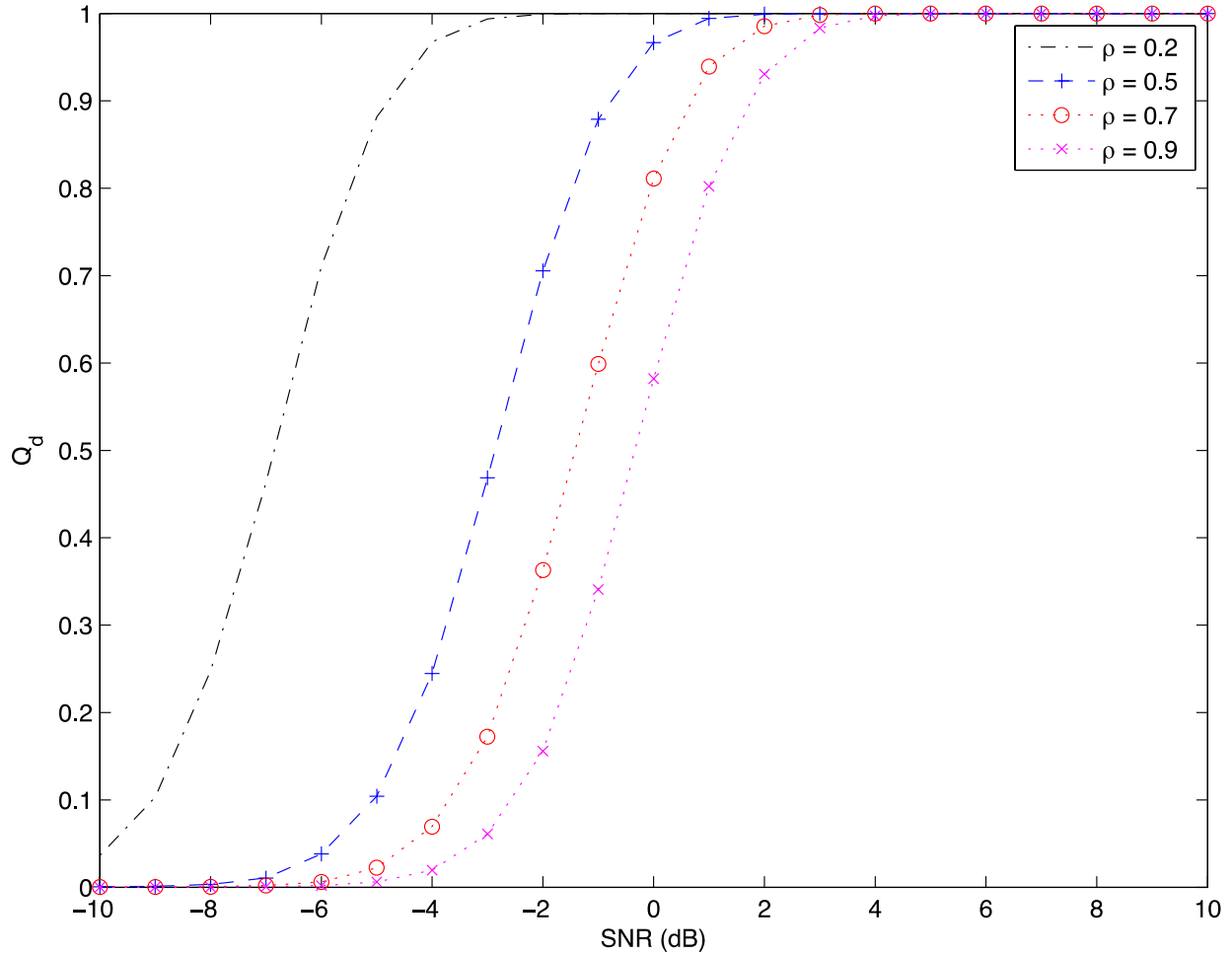


Fig. 15.  $Q_d$  vs. SNR for different  $\rho$  in cooperative spectrum sensing with  $N$  of 10,  $\lambda = 6.9$  and  $p = 4$ .

### 3.5 Conclusion

In this chapter, the sensing performance of IED in Rayleigh fading is studied under the influence of noise variance uncertainty. Interestingly, to improve the performance of IED adaptive tuning of IED parameter  $p$  is required and optimal value of  $p$  depends on detection threshold, samples size, SNR values and the degree of noise variance uncertainty. Further, to enhance the sensing performance, a network of cooperating CRs each equipped with an IED is considered by deploying MAJORITY fusion rule to combine the individual CR decisions at the FC. Surprisingly, increasing the number of CRs does not necessarily improve the detection performance and the optimal number of CRs depends upon the choice of  $p$  in addition to the aforementioned parameters of interest. Thus, a careful selection of the number of CRs and IED parameter  $p$  would be needed to yield meaningful performance gains.

## Chapter 4

### Conclusion and Future Work

In this research project, the problem of spectrum sensing in CR networks was investigated by using an IED. First, spectrum sensing with a single CR equipped with an improved energy detector was considered in the Rayleigh fading channel and with uncertain noise variance. The IED, which is a more generalized version of the traditional energy detector, was found to yield significant performance gains compared to the performance of the traditional energy detector after fine tuning the parameter  $p$  (which is a constant; i.e.,  $p = 2$  for the conventional energy detector) in environments with uncertain noise variance. The degradation in spectrum sensing performance with the increase in noise variance uncertainty was found to be mitigated substantially by adaptive tuning of the parameter  $p$ . Motivated by the improved performance, and in order to further enhance the spectrum sensing reliability, we considered a cooperative network of several CRs equipped with the improved energy detector by utilizing the MAJORITY fusion rule at the fusion center. Interestingly, encouraging performance gains compared to the performance of single CR-based spectrum sensing were observed, demonstrating that cooperation combined with the use of improved energy detector effectively mitigated the problem of noise variance uncertainty in the conventional energy detector.

Extending this project to scenarios with different fading channels models, for instance, Nakagami- $m$  and/or Rician fading, would be interesting in order to study the impact of different degrees of wireless multipath fading on the detection performance of the improved energy detector under noise variance uncertainty. Another interesting extension would be to consider the channel estimation errors in addition to the noise variance uncertainty and its effect on the sensing quality of the improved energy detector. Further extension of both of these scenarios to cooperative spectrum sensing might be interesting to study and quantify the achievable performance gain due to cooperative diversity.

## References

- [1] FCC, Spectrum Policy Task Force, [ET Docket 02-135, Nov. 2002].
- [2] M. A. McHenry, BNSF spectrum occupancy measurements project summary, [Shared Spectrum Company Rep., Aug. 2005].
- [3] M. McHenry, E. Livsics, T. Nguyen, and N. Majumdar, BXG dynamic spectrum access field test results, *IEEE Comm. Mag.*, vol. 45, Jun. 2007, pp. 5157.
- [4] Khaled Ben Letaiff, Wei Zhang, "Cooperative Communications for Cognitive Networks", *IEEE Proc.* Vol. 97, No. 5, pp.878,893, May 2009.
- [5] Rahul Tandra, Shridhar Mubaraq, Mishra Anant Sahai, "What is a spectrum hole and what does it take to recognize one?" [online] Available on url <http://www.eecs.berkeley.edu/~sahai/Papers/SpectrumHolesProcIEEE.pdf>
- [6] Yunfei Chen, "Improved Energy Detector for random signal in Gaussian Noise", *IEEE Trans. on Wireless Comm.*, vol. 9, No. 2, February 2010.
- [7] Gordon L. Stuber "Principles of Mobile Communications", second edition, 2002, kluwer academic publishers.
- [8] Peh, E. and Y. C. Liang, "Optimization for Cooperative Sensing in Cognitive Radio Networks", *Proc. Wireless Comm. Networking Conf. (WCNC)*, 2007, pp. 27–32.
- [9] S. Haykin, "Cognitive radio: brain-empowered wireless communications", *IEEE J. Select. Areas in Comm.* 2005.
- [10] Urkowitz, Harry, "Energy detection of unknown deterministic signals," *IEEE Proc.*, vol.55, no.4, pp.523,531 April 1967.
- [11] "Tuna Tuğcu." *Tuna Tuğcu*. Web. 23 Jan. 2014, [online], Available on <http://www.cmpe.boun.edu.tr/~tugcu/res>.
- [12] "Mobile Data Traffic Predictions Say: It's WiFi Offload!" *Frank Rayal*. Web. 23 Jan. 2014, [online], Available on <http://frankrayal.com/2013/03/20/mobile-data-predictions-say-its-wifi-offload>
- [13] R. Tandra and A. Sahai, "SNR Walls for Signal Detection," *IEEE J. Select. Topics Sig. Pro.*, vol. 2, 2008, pp. 4-17.
- [14] Mishra, S.M.; Sahai, A.; Brodersen, R.W., "Cooperative Sensing among Cognitive Radios," *IEEE Int. Conf. on Comm.*, June 2006.

- [15] P. Beckmann and A. Spizzichino, *The Scattering of Electromagnetic Waves from Rough Surfaces*, 2nd ed., Boston, MA: Artech House, 1987.
- [16] Zhu Han; Rongfei Fan; Hai Jiang, "Replacement of spectrum sensing in cognitive radio," *IEEE Trans. Wireless Comm.*, vol.8, no.6, pp.2819, 2826, June 2009.
- [17] "Join Academia.edu & Share your research with the world." *Noise uncertainty in cognitive radio sensing: analytical modeling and detection performance*. Web. 23 Jan. 2014. [Online] Available on [http://www.academia.edu/1906594/Noise\\_uncertainty\\_in\\_cognitive\\_radio\\_sensing\\_analytical\\_modeling\\_and\\_detection\\_performance](http://www.academia.edu/1906594/Noise_uncertainty_in_cognitive_radio_sensing_analytical_modeling_and_detection_performance).
- [18] Kostylev, V.I., "Energy detection of a signal with random amplitude," *IEEE Int. Conf. on Comm.*, 2002.
- [19] Digham, F.F.; Alouini, M.-S.; Simon, Marvin K., "On the energy detection of unknown signals over fading channels," *IEEE Int. Conf. on Comm.*, 11-15 May 2003.
- [20] Cabric, D.; Mishra, S.M.; Brodersen, R.W., "Implementation issues in spectrum sensing for cognitive radios," *Conf. on Sig. Sys and Comm.*, vol.1, 7-10 Nov. 2004.
- [21] E. Visotsky, S. Kuffner, and R. Peterson, "On collaborative detection of TV transmissions in support of dynamic spectrum sharing," *IEEE Int. Symp. On New Frontiers in Dynamic Spectrum Access Networks*, pp. 338-345, Nov. 2005.
- [22] Wei Lin; Qinyu Zhang, "A design of energy detector in cognitive radio under noise uncertainty," *IEEE Singapore Int. Conf. on Comm. Sys.*, 2008, pp.213, 217, Nov. 2008.
- [23] Eghbali, Y.; Hassani, H.; Attari, M.A., "Cooperative spectrum sensing by improved energy detector for heterogeneous environments in cognitive radio networks," *2012 Sixth Int. Sym. Telecomm. (IST)*, 6-8 Nov. 2012, pp.383, 386.
- [24] Singh, Ajay; Bhatnagar, Manav R.; Mallik, Ranjan K., "Performance analysis of multiple sample based improved energy detector in collaborative CR networks," *2013 IEEE 24th Int. Sym. on Personal Indoor and Mobile Radio Comm.*, pp.2728,2732, 8-11 Sept. 2013.
- [25] Teguig, D.; Scheers, B.; Le Nir, V., "Data fusion schemes for cooperative spectrum sensing in cognitive radio networks," *Comm. and Info. Sys. Conf.*, 8-9 Oct. 2012.
- [26] Digham, F.F., "Optimum Energy-Delay Tradeoffs for Distributed Detection in Wireless Sensor Networks," *IEEE International Symposium on Sig. Pro. Info. Tech.*, pp.208,213, 15-18 Dec. 2007.

- [27] Herath, S.P.; Rajatheva, N.; Tellambura, C., "On the energy detection of unknown deterministic signal over Nakagami channels with selection combining," *Canadian Conf. on Electrical and Computer Engineering.*, 3-6 May 2009.
- [28] Atapattu, S.; Tellambura, C.; Hai Jiang, "Energy Detection Based Cooperative Spectrum Sensing in Cognitive Radio Networks," *IEEE Trans. on Wireless Comm.*, vol.10, no.4, pp.1232,1241, April 2011.
- [29] Tandra, R.; Sahai, A., "Noise Calibration, Delay Coherence and SNR Walls for Signal Detection," *IEEE Symp. on New Frontiers in Dynamic Spectrum Access Networks*, pp.1,11, 14-17 Oct. 2008.